



## Article

# Investigating Scattering Spectral Characteristics of GaAs Solar Cells by Nanosecond Pulse Laser Irradiation

Hao Chang , Weijing Zhou , Zhilong Jian, Can Xu, Yingjie Ma and Chenyu Xiao

Department of Aerospace Science and Technology, Space Engineering University, Beijing 101416, China; changhao5976911@163.com (H.C.); jzl862366@163.com (Z.J.); mayingjie@hgd.edu.cn (Y.M.); 16605655985@163.com (C.X.)

\* Correspondence: viviazhouy@163.com

## Abstract

Reliable power generation from solar cells is critical for spacecraft operation. High-energy laser irradiation poses a significant threat, as it can potentially cause irreversible damage to solar cells, which is difficult to detect remotely using conventional techniques such as radar or optical imaging. Spectral detection offers a potential approach through unique “spectral fingerprints,” but the spectral characteristics of laser-damaged solar cells remain insufficiently documented. This study investigates the scattering spectral characteristics of triple-junction GaAs (Gallium Arsenide) solar cells subjected to nanosecond pulsed laser irradiation to establish spectral signatures for damage assessment. GaAs solar cells were irradiated at varying energy densities. Bidirectional Reflectance Distribution Function (BRDF) spectra (400–1200 nm) were measured. A thin-film interference model was used to simulate damage effects by varying layer thicknesses, thereby interpreting experimental results. The results demonstrate that as the laser energy density increases from 0.12 to 2.96 J/cm<sup>2</sup>, the number of absorption peaks in the visible range (400–750 nm) decreases from three to zero, and the oscillation in the near-infrared range vanishes completely, indicating progressive damage to the GaInP (Gallium Indium Phosphide) and GaAs layers. This study provides a spectral-based approach for remote assessment of laser-induced damage to solar cells, which is crucial for satellite health monitoring.



Academic Editor: Hyun-Ung Oh

Received: 27 July 2025

Revised: 3 October 2025

Accepted: 9 October 2025

Published: 10 October 2025

**Citation:** Chang, H.; Zhou, W.; Jian, Z.; Xu, C.; Ma, Y.; Xiao, C.

Investigating Scattering Spectral Characteristics of GaAs Solar Cells by Nanosecond Pulse Laser Irradiation. *Aerospace* **2025**, *12*, 909. <https://doi.org/10.3390/aerospace12100909>

**Copyright:** © 2025 by the authors. Licensee MDPI, Basel, Switzerland. This article is an open access article distributed under the terms and conditions of the Creative Commons Attribution (CC BY) license (<https://creativecommons.org/licenses/by/4.0/>).

**Keywords:** nanosecond laser irradiation; solar cells; scattering spectrum; satellite health monitoring; damage assessment

## 1. Introduction

Spacecraft, the vanguards of exploration, communication, and observation beyond Earth’s atmosphere, are critically dependent on a consistent and reliable power supply to maintain their operational integrity and fulfill their mission objectives. Solar cells, which convert sunlight directly into electricity, have long served as the primary power source for the vast majority of satellites and interplanetary probes, owing to their durability, relatively high efficiency, and the inexhaustible nature of solar energy in space. The performance and longevity of these photovoltaic arrays are paramount, as any degradation or failure can lead to diminished operational capabilities or even complete mission failure. While solar cells are essential for spacecraft power, they are vulnerable to high-energy lasers when transmitting laser power. Therefore, developing reliable remote detection methods for laser-induced damage is of paramount importance.

While low-power laser irradiation might temporarily affect the cell's output performance, high-energy laser pulses can induce irreversible physical damage [1,2]. This phenomenon is not limited to a specific cell technology and has been observed across various photovoltaic devices. For instance, studies on silicon solar cells have documented the degradation of electrical parameters following nanosecond pulse laser irradiation [3]. Furthermore, research on high-efficiency multi-junction cells has explored strategies like top-hat beam ablation to modify the nature of laser-induced damage [4]. These independent studies corroborate the significant threat posed by high-energy lasers and underscore the importance of developing reliable damage assessment techniques. The ability to detect and characterize such damage remotely is therefore of significant interest for satellite health monitoring. Traditional detection techniques, such as radar and conventional optical imaging, face substantial challenges in detecting and characterizing laser-induced damage on solar cells. Radar systems, while effective for tracking and orbit determination, typically lack the resolution to identify surface damage on solar cells [5]. Standard optical imaging, though capable of providing visual information, may struggle to resolve the changes caused by laser damage, especially given the vast distances involved and atmospheric distortions associated with ground-based observations. Therefore, these methods may not provide sufficient information to assess the nature or extent of the damage, which is crucial for understanding the impact of lasers on solar cell performance.

In recent years, spectral detection technology has emerged as a powerful and versatile tool in various applications, including the identification and characterization of space targets. This technology operates on the principle that different materials interact with electromagnetic radiation in unique ways, absorbing, reflecting, or emitting light at specific wavelengths. By capturing and analyzing the spectrum of light reflected or emitted from a target, it is possible to obtain wavelength-resolved information that acts as a "spectral fingerprint" [6,7]. The physical basis for using spectral detection to identify laser-damaged solar cells lies in the material changes that occur upon irradiation. Laser energy absorption leads to a significant temperature rise. This thermal damage can alter the optical properties of the various layers constituting a modern solar cell. Therefore, laser-induced damage is expected to produce detectable shifts in the cell's spectral signature, providing a foundation for remote damage assessment.

The investigation of scattering spectral characteristics of space targets is not a new endeavor. Early pioneering work by researchers such as Jorgenson [8] involved measuring the scattering spectra of over three hundred common space target materials, leading to the establishment of a valuable spectral database for material identification. This foundational work paved the way for subsequent studies. For example, Jorgenson et al. [9] successfully identified the materials of rocket bodies and satellites by analyzing their scattering spectral curves in the 0.3 to 0.9  $\mu\text{m}$  wavelength range. These studies demonstrated the potential of reflectance spectroscopy for non-invasively determining the material composition of orbital objects. Further advancements in this field have involved more detailed characterization of specific materials and the analysis of more complex spectral phenomena. Bedard and Lévesque analyzed the spectral reflectance measurements of the CanX-1 engineering model of the satellite, explaining the observed scattering spectral curve and investigating the impact of measurement model changes on the results. Bedard [10] also characterized specific spacecraft materials using BRDF, and, in a later study, Bedard and Wade [11,12] utilized time-resolved visible/near-infrared spectrometric observations to identify the material composition of the Galaxy-11 geostationary satellite through telescopic measurements.

Concurrently, specific research has also been directed towards understanding the spectral characteristics of solar cells themselves. In our previous research, the scattering spectral characteristics of triple-junction GaAs solar cells were simulated, and the impact of internal structure on the reflectance of scattering spectra was examined [13]. The findings revealed that the GaInP layer and GaAs layer play a significant role in shaping the scattering spectra curve within the structure of triple-junction GaAs solar cells. Specifically, the GaInP layer affected the absorption properties in the visible spectrum range, while the GaAs layer influenced the oscillation curves in the near-infrared spectrum range.

It is noteworthy that the in-depth study of GaAs cell optical properties has long focused on actively controlling their reflection and scattering behavior through advanced methods such as nanostructured gratings to maximize conversion efficiency [14–16]. For example, Das et al. systematically studied anti-reflection gratings for highly efficient next-generation GaAs cells [14] and optimized their design [15], while Nur-E-Alam et al. provided a comprehensive review of efficiency enhancement via nanostructures [16]. In contrast to this prior focus on performance optimization, our study pivots towards damage diagnosis. While previous studies have focused on the spectral characteristics of intact solar cells or the general effects of laser irradiation, there is a notable lack of research quantitatively linking specific laser energy densities to layer-by-layer spectral damage signatures in triple-junction GaAs cells. Our work fills this gap by establishing a direct correlation between nanosecond pulsed laser energy density and quantifiable changes in the BRDF, providing a novel methodology for remote damage diagnostics. We examined the impacts of varying laser densities on the cell's BRDF. Furthermore, by employing a cell scattering spectral model rooted in thin film interference theory, we also delved into the alterations in absorption peaks in the visible spectrum and the changes in oscillation observed in the near-infrared spectrum. The insights gained from this combined experimental and theoretical approach are expected to elucidate the mechanisms by which laser damage alters the spectral response of triple-junction GaAs solar cells.

## 2. Damage Testing by Nanosecond Pulse Laser Irradiation

The GaAs solar cell with a surface size of  $10 \times 10$  mm was irradiated by a laser beam with a diameter of approximately 5 mm, a wavelength of 1064 nm, and a pulse width of 10 ns. The laser energy density was varied by changing the energy of the laser. All solar cell samples were obtained from the same production batch to ensure consistency. Prior to laser irradiation and spectral measurement, each cell was cleaned using an ultrasonic cleaner with ethanol to remove surface contaminants. Laser energy densities of 0.12, 0.42, 1.16, 1.58, 2.14, and 2.96 J/cm<sup>2</sup> were used to irradiate the cells, causing visible damage on the surface. As shown in Figure 1, when the irradiation laser energy density is 0.12 and 0.42 J/cm<sup>2</sup>, there is no significant change on the surface of the cell; however, when the irradiation laser energy density is 1.16 J/cm<sup>2</sup>, damage is observed on the surface, with some silver-colored ablative areas appearing at the irradiation site. With the increase in laser energy density, the damage becomes more pronounced, as seen when the irradiation laser energy densities are 1.58, 2.14, and 2.96 J/cm<sup>2</sup>, where distinct damage areas are visible.

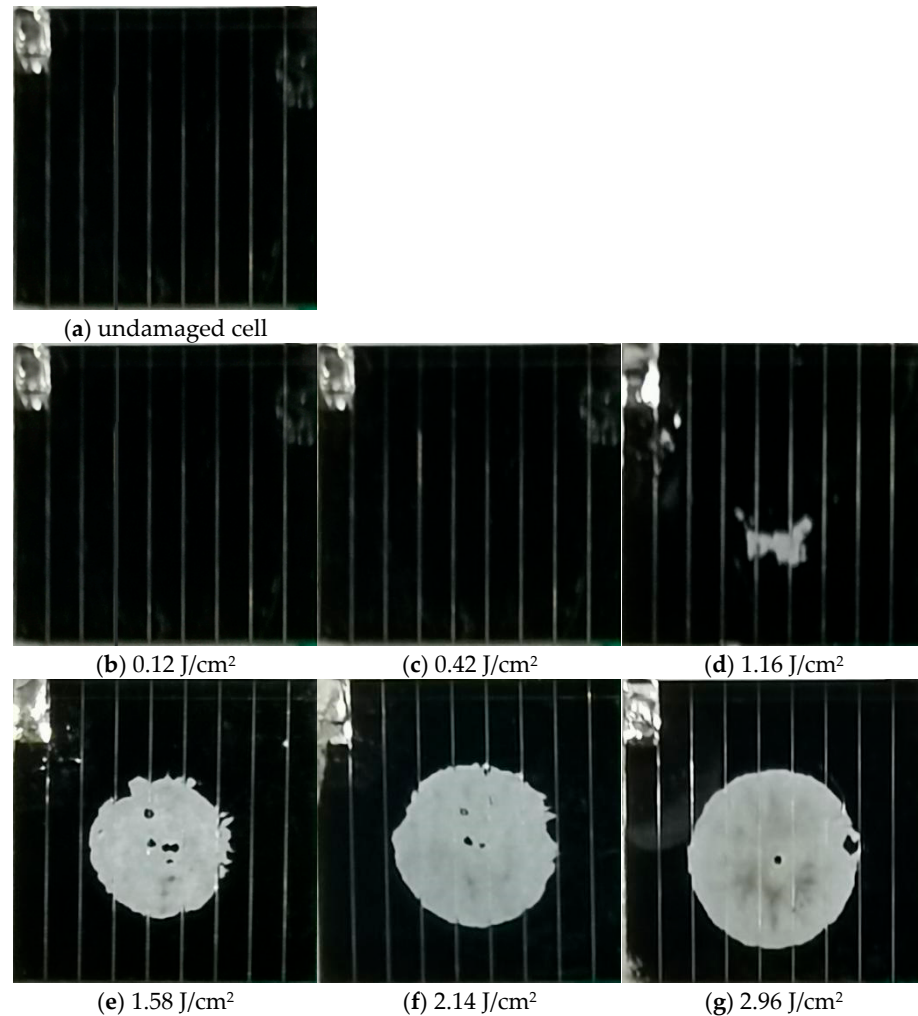


**Figure 1.** Surface morphology of the solar cells before and after laser irradiation with different laser densities.

### 3. Scattering Spectra Measurements and Results

#### 3.1. BRDF Measurement Setup

A schematic diagram of the experimental setup for BRDF measurement is provided in Figure 2. The setup primarily consists of a broadband light source, a goniometric stage for precise control of incidence and observation angles, and a spectrometer coupled with a detector [2]. The cell sample was mounted at the center of the stage. The incident angle ( $\theta_i$ ) was fixed at  $30^\circ$ , and the scattered light was collected at a detection angle ( $\theta_r$ ) of  $30^\circ$ , which was chosen as a representative angle for analyzing the specular–diffuse scattering components. The BRDF was calculated as the ratio of the scattered radiance to the incident irradiance at each wavelength. To ensure measurement accuracy and quantify experimental uncertainty, the BRDF measurement system was calibrated using a standard reference panel (Spectralon®). The relative uncertainty of the BRDF measurements was estimated to be within  $\pm 5\%$ , based on repeated measurements of the reference standard under the same geometric conditions. Each laser energy condition was tested on three separate cell samples, and BRDF measurements were repeated three times per sample. The results presented are the average of these replicates. The overall research process comprised the following sequential stages: Sample Preparation → Laser Irradiation (with varying energy densities) → Surface Morphology Analysis → BRDF Spectral Measurement →

Data Analysis. This structured approach ensured a systematic investigation from inducing damage to interpreting its spectral signatures.

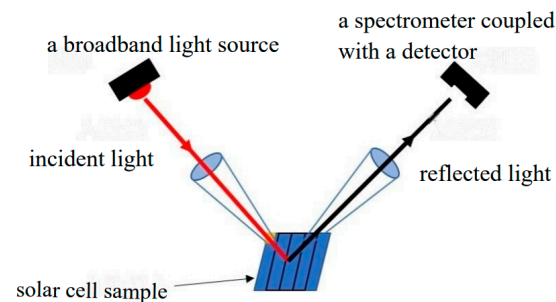


**Figure 2.** A schematic diagram of the BRDF measurement setup.

The spectral range of 400–1200 nm was strategically selected for two primary reasons [2,7]. Firstly, it encompasses the characteristic absorption bands and interference features of the key functional layers within the triple-junction GaAs solar cell. Specifically, the GaInP top cell primarily absorbs light in the visible range (400–750 nm), and its thickness governs the interference-induced absorption peaks observed between 600 and 750 nm. The GaAs middle cell is active in the near-infrared range (900–1200 nm), and its thicker layer is responsible for the distinct oscillation patterns seen beyond 900 nm. The Ge bottom cell has a cutoff wavelength near 1800 nm; however, our upper limit of 1200 nm is sufficient to capture the critical transition region where the oscillations from the GaAs layer diminish, which is a key indicator of damage. Secondly, this range allows us to simultaneously monitor the laser-induced degradation of both the visible-range absorption peaks (related to the GaInP layer) and the near-infrared oscillations (related to the GaAs layer), providing a comprehensive spectral fingerprint for damage assessment. Wavelengths below 400 nm are strongly absorbed by the DAR layer and substrate, while those beyond 1200 nm are dominated by the Ge substrate and contribute little to the layer-specific spectral features under investigation. Therefore, the spectral range of 400–1200 nm was selected because it covers the primary optical response and interference features of the GaInP and GaAs layers. The BRDF measurement offers a significant advantage for this study as it provides wavelength-resolved information about the surface’s scattering properties under specific geometric conditions. Unlike simple reflectance measurements, BRDF captures both specular and diffuse components, making it highly sensitive to subtle changes in surface morphology and layer optical properties induced by laser damage. This allows for a more comprehensive fingerprint of the damage state than total reflectance alone.

### 3.2. Results

The BRDF curves of the solar cells irradiated with different laser energy densities are shown in Figure 3. When the laser energy density is 0.12 and 0.42 J/cm<sup>2</sup>, the BRDF of the visible and near-infrared spectral ranges of the cell are shown in Figure 3a–d. Under pulsed laser irradiation, the number of absorption peaks in the 600–750 nm visible spectral range decreases, and the amplitude of absorption peaks weakens compared to the original intact cell. The amplitude of the curve in the near-infrared spectral range also decreases, but oscillation phenomena persist. When the laser energy density is 1.16 J/cm<sup>2</sup>, damaged areas appear on the cell surface. The amplitude of absorption peaks significantly decreases, and the oscillation phenomena in the near-infrared spectral range disappear. With further increase in laser energy density (1.58, 2.14, and 2.96 J/cm<sup>2</sup>), the degree of cell damage intensifies, leading to a significant decrease in the curve amplitude in the visible spectral range, disappearance of absorption peak characteristics in the visible wavelength range, and complete disappearance of oscillation in the near-infrared spectral range.



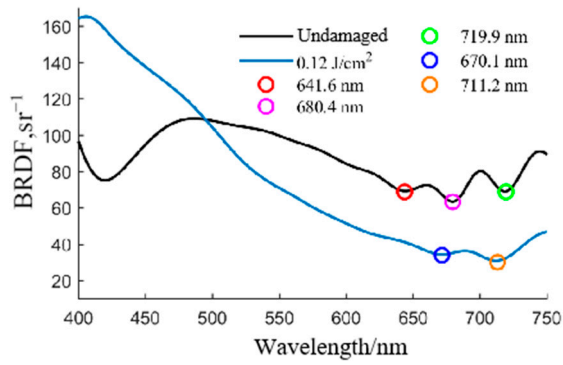
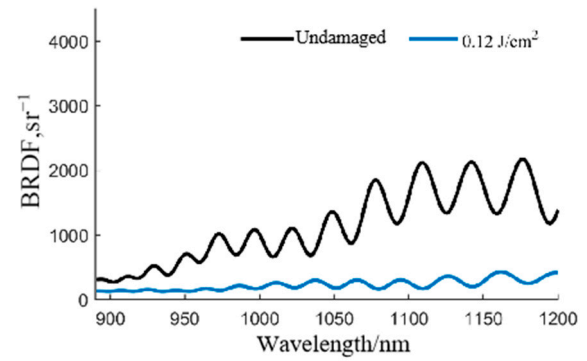
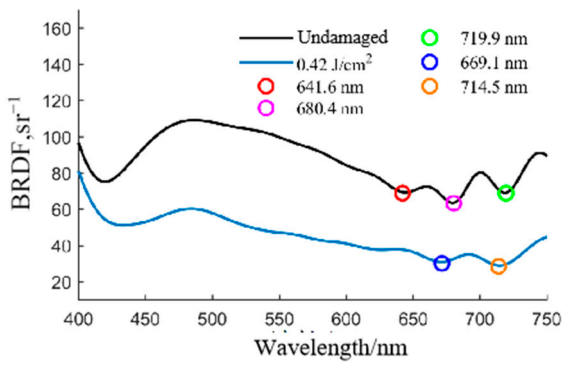
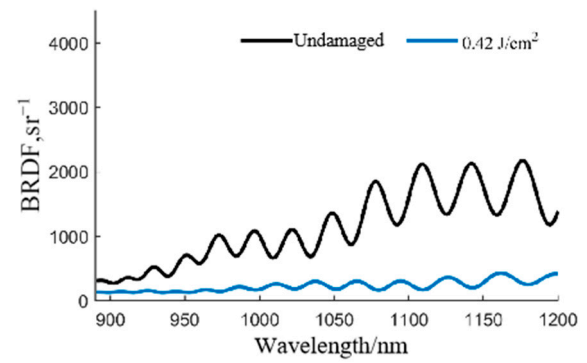
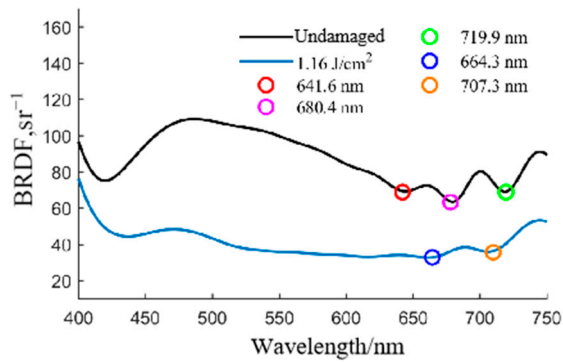
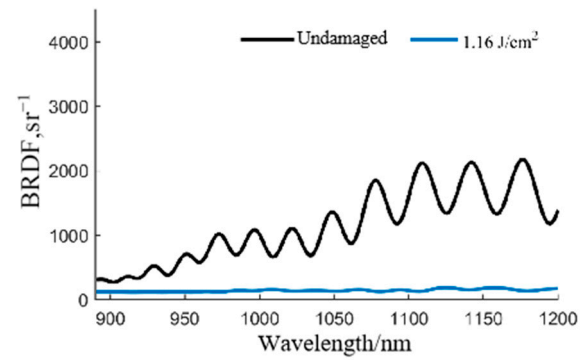
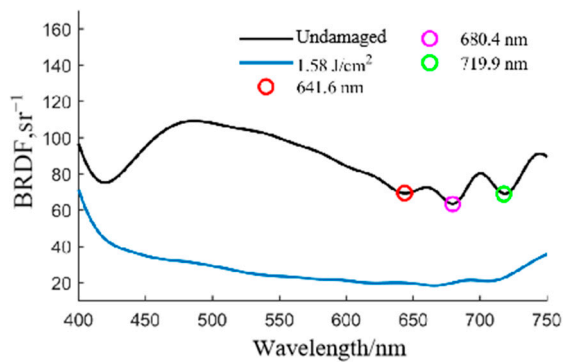
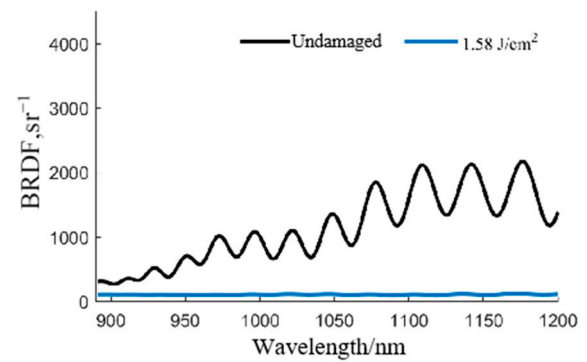
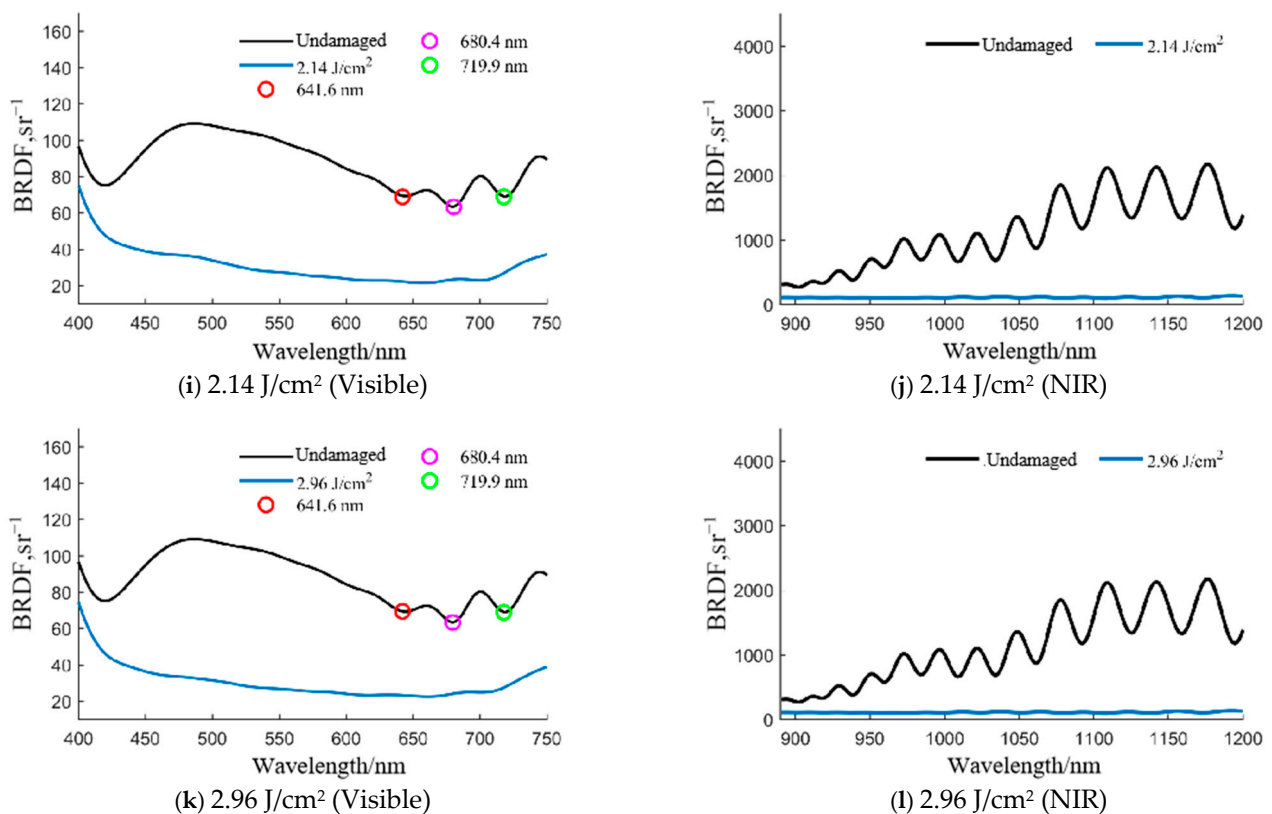
(a) 0.12 J/cm<sup>2</sup> (Visible)(b) 0.12 J/cm<sup>2</sup> (NIR)(c) 0.42 J/cm<sup>2</sup> (Visible)(d) 0.42 J/cm<sup>2</sup> (NIR)(e) 1.16 J/cm<sup>2</sup> (Visible)(f) 1.16 J/cm<sup>2</sup> (NIR)(g) 1.58 J/cm<sup>2</sup> (Visible)(h) 1.58 J/cm<sup>2</sup> (NIR)

Figure 3. Cont.



**Figure 3.** Experimental BRDF measurement results for solar cells irradiated with various laser energy densities. For each energy density, the left panel (a,c,e,g,i,k) shows the spectral characteristics in the visible range (400–750 nm), while the right panel (b,d,f,h,j,l) shows the corresponding characteristics in the near-infrared range (900–1200 nm).

#### 4. Analysis

Based on experimental results, a model that we had previously established, rooted in thin film interference theory [11], was employed to study the impact of damage to different layers of a triple-junction GaAs solar cell on its spectral reflectance characteristics. After laser damage, the spectral reflectance of the individual cell layers at different thicknesses was analyzed. In the GaAs solar cell, the anti-reflection coating (DAR) layer and the bottom Ge (Germanium) layer mainly absorb light and have minimal impact on the cell's scattering spectral characteristics. In the case of single-layer cell structures, the scattering spectra of GaInP and GaAs cell layers of different thicknesses by laser damage are shown in Figure 4.

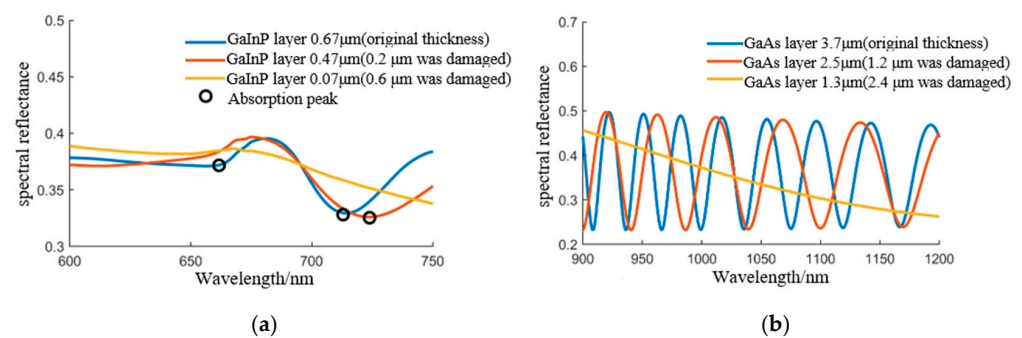


**Figure 4.** Impact of variations in the thickness of the GaInP and GaAs layers on the spectral reflectance characteristics. (a) GaInP layer (b) GaAs layer.

From Figure 4, it can be seen that, when the GaInP layer is intact (original thickness is  $0.67\text{ }\mu\text{m}$ ), there are three absorption peaks in the visible spectrum range of  $600\sim 750\text{ nm}$ ; and when the GaAs layer is intact (original thickness is  $3.7\text{ }\mu\text{m}$ ), there are oscillations in the near-infrared spectrum range. As the thickness of the GaInP layer decreases, the number of absorption peaks in the visible spectrum range decreases, and the peak amplitude decreases; for example, when the GaInP layer's laser damage thickness decreases to  $0.47\text{ }\mu\text{m}$ , only one absorption peak is visible in the visible light range. When the laser damage thickness decreases to  $0.07\text{ }\mu\text{m}$ , the absorption peak in the visible light range completely disappears. Similarly, as the thickness of the GaAs layer decreases, the oscillation gradually disappears.

Utilizing the changes in the thickness of the GaInP layer and the GaAs layer of the solar cell to characterize the damage, the laser-induced thickness changes in the GaInP layer and the GaAs layer were obtained through simulations of various conditions based on scattering spectroscopy measurement data. Figure 5 shows the characteristics of the GaInP layer and GaAs layer thickness changes caused by variations in laser energy densities. The horizontal axis represents the laser energy density, the left vertical axis represents the GaInP layer thickness, and the right vertical axis represents the GaAs layer thickness. The black line represents the change in GaInP layer thickness, and the red line represents the change in GaAs layer thickness.

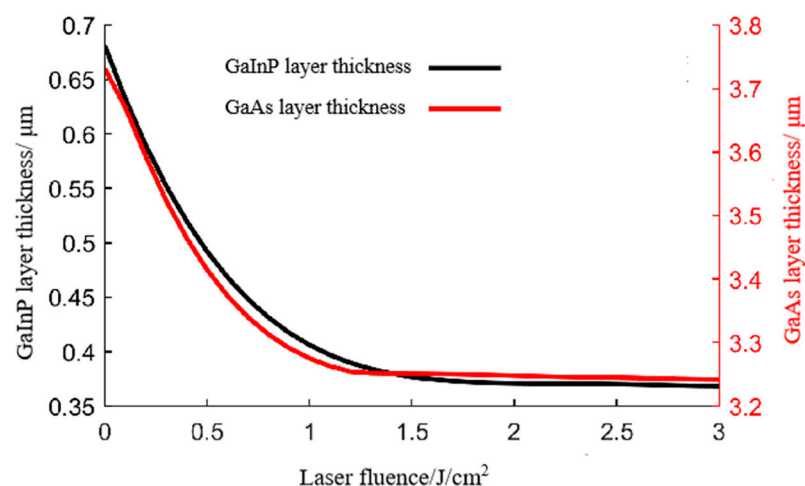


**Figure 5.** Thickness variations in the GaInP layer and GaAs layer under pulsed laser irradiation.

Based on the thickness changes obtained from Figure 5, further simulations were conducted to obtain the BRDF changes in the solar cell after irradiation with different laser energy densities, which were then compared with measurement results, as shown in Figure 6. The black line in the figure represents the measurement BRDF of the original intact cell, the blue line represents the measurement BRDF of the irradiated damaged cell, and the red line represents the simulated results. A visual comparison reveals that the simulated spectral curves capture the key experimental trends, namely the reduction in the number of visible-range absorption peaks and the damping of near-infrared oscillations with increasing laser energy density. When the irradiation laser energy density is less than  $1.16\text{ J}/\text{cm}^2$ , the absorption peaks in the visible spectrum range and the oscillation in the near-infrared spectral range still exist as the laser energy density increases, with only changes in amplitude, indicating minimal damage to the GaInP and GaAs layers. When the irradiation laser energy density is greater than  $1.58\text{ J}/\text{cm}^2$ , the amplitude of the visible light spectrum curve decreases significantly with increasing laser energy density, making it difficult to observe absorption peaks. At the same time, the oscillation curve in the near-infrared spectral range disappears completely, reflecting significant damage to the GaInP and GaAs layers of the cell. These spectral changes occur because when a  $1064\text{ nm}$



wavelength nanosecond pulsed laser irradiates a triple-junction GaAs solar cell, the photon energy of the laser does not reach the bandgap widths of the top GaInP layer and middle GaAs layer of the cell, allowing the laser to penetrate through the GaInP and GaAs layers to reach the Ge layer. Nanosecond pulsed lasers have extremely high peak power densities, causing the GaAs layer adjacent to the Ge layer to be damaged first, leading to the gradual disappearance of the oscillation in the near-infrared spectral range. With increasing laser energy density, i.e., when the laser energy density is greater than  $1.58 \text{ J/cm}^2$ , the damage to the GaAs layer adjacent to the Ge layer increases due to the high peak power density of the acting laser, as well as a gradual expanding increase in damage to the GaInP layer, resulting in the visible light absorption peak characteristics tending to disappear in the scattered spectrum features.

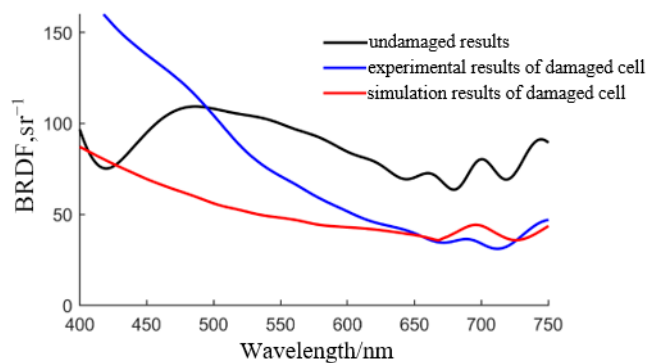
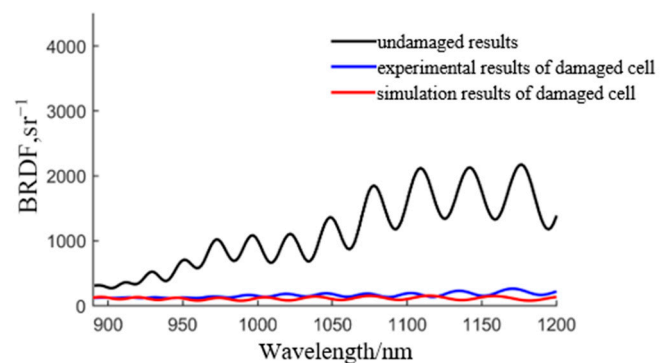
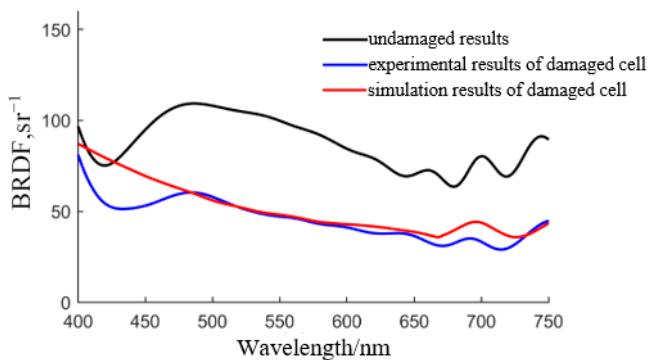
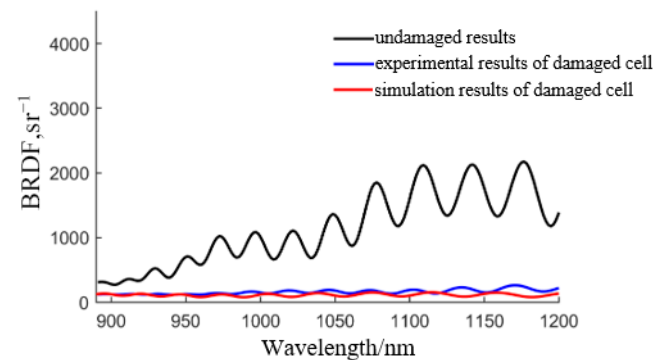
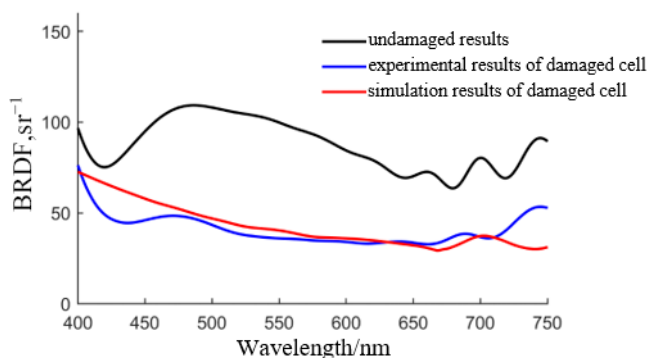
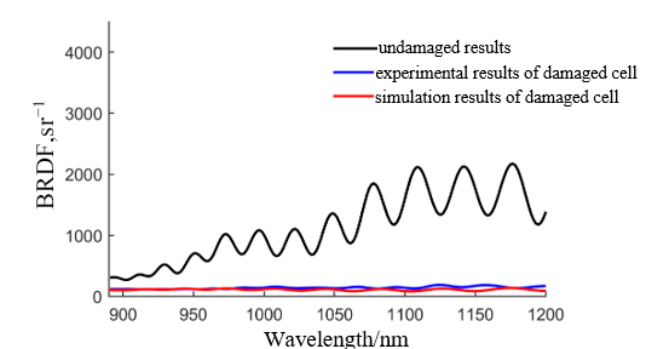
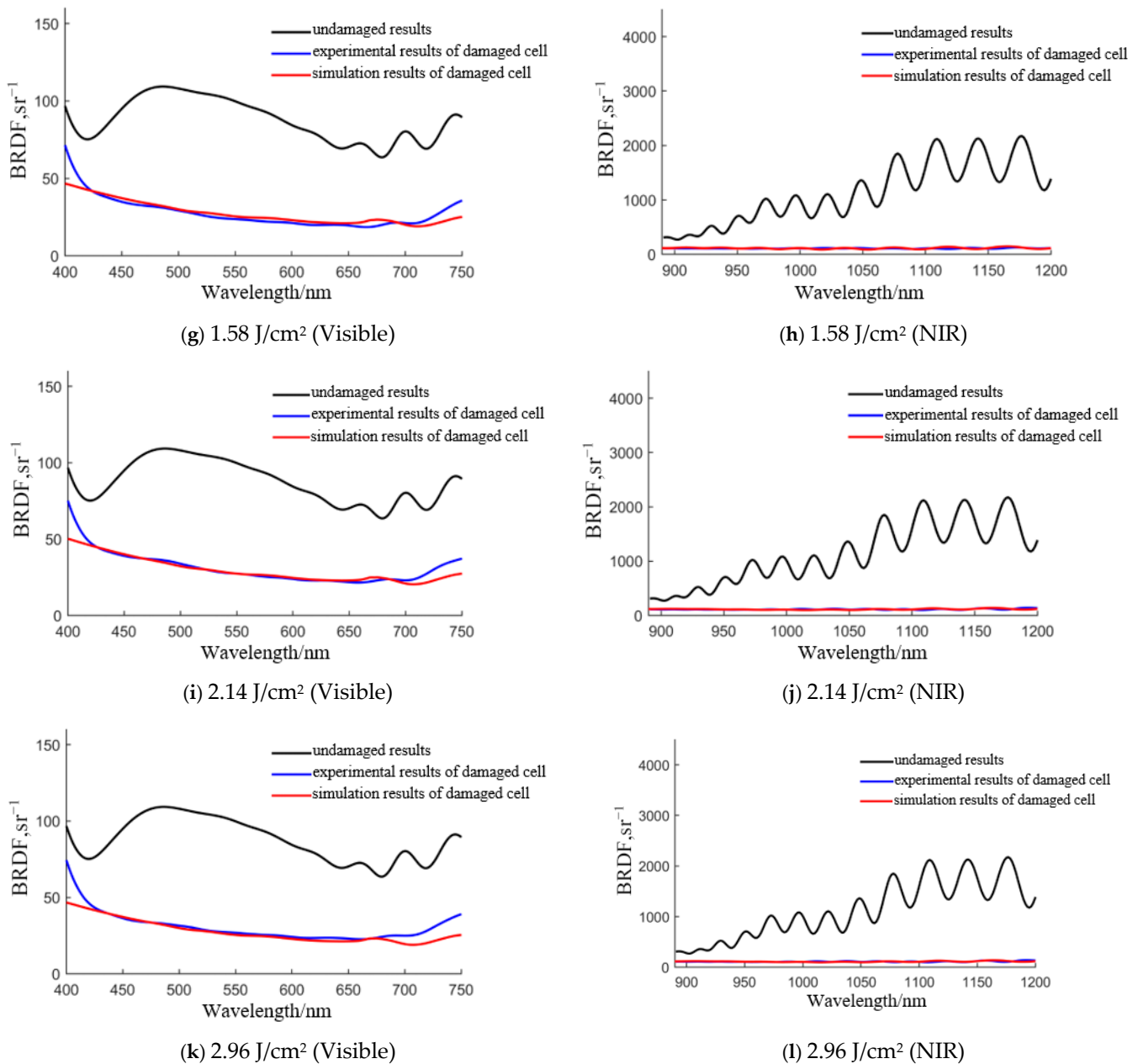
(a)  $0.12 \text{ J/cm}^2$  (Visible)(b)  $0.12 \text{ J/cm}^2$  (NIR)(c)  $0.42 \text{ J/cm}^2$  (Visible)(d)  $0.42 \text{ J/cm}^2$  (NIR)(e)  $1.16 \text{ J/cm}^2$  (Visible)(f)  $1.16 \text{ J/cm}^2$  (NIR)

Figure 6. Cont.



**Figure 6.** Comparison of the simulation results and experimental measurements of the cell's BRDF irradiated under different laser densities. For each energy density, the left panel (a,c,e,g,i,k) shows the spectral characteristics in the visible range (400–750 nm), while the right panel (b,d,f,h,j,l) shows the corresponding characteristics in the near-infrared range (900–1200 nm).

To systematically summarize the damage rules revealed by the experiment-simulation comparison in Figure 6, the key BRDF spectral characteristics, their corresponding simulated layer thickness variations, and the associated damage levels are synthesized in Table 1. This table not only quantifies the evolution of spectral features but, more importantly, establishes a direct link between the macroscopic spectral shifts and the microscopic physical damage (i.e., the thinning of the GaInP and GaAs layers) through our model simulations.

**Table 1.** Correlation between laser energy density, experimental BRDF characteristics, simulated layer damage, and assessed damage level based on the experiment-simulation comparison in Figure 6.

Laser Energy Density (J/cm <sup>2</sup> )	Key Experimental BRDF Changes	Simulated Layer Thickness (vs. Intact)	Assessed Damage Level
0 (Intact)	Visible: Three distinct absorption peaks. NIR: Pronounced oscillation.	GaInP: ~0.67 $\mu\text{m}$ ; GaAs: ~3.7 $\mu\text{m}$	None (Baseline)
0.12–0.42	Visible: Number of peaks decreases; amplitude weakens. NIR: Oscillation amplitude decreases.	GaInP: ~0.5 $\mu\text{m}$ ; GaAs: ~3.5 $\mu\text{m}$	Mild
1.16	Visible: Peak number/position stable; amplitude drops significantly. NIR: Oscillation disappears.	GaInP: ~0.41 $\mu\text{m}$ ; GaAs: ~3.25 $\mu\text{m}$	Moderate
1.58–2.96	Visible: Absorption peaks disappear. NIR: Oscillation disappears.	GaInP: ~0.36 $\mu\text{m}$ ; GaAs: ~3.23 $\mu\text{m}$	Severe

As presented in Table 1, a high degree of consistency is observed between the experimental measurements and the model simulations regarding the evolution of key spectral characteristics. This agreement confirms that the absorption peak features in the visible range are primarily governed by the thickness of the GaInP layer, while the oscillation characteristics in the NIR range are dominated by the GaAs layer. Consequently, we have established a spectral fingerprint-based criterion for damage assessment: Moderate damage is identified when the NIR oscillations vanish completely, coupled with a reduction in visible absorption peaks; Severe damage is indicated by the complete disappearance of the absorption peaks (signifying severe damage to the GaInP layer). Despite this good qualitative agreement, it is important to acknowledge the limitations of the employed model. The thin-film interference model assumes ideal layer uniformity and does not account for lateral inhomogeneity or complex damage morphologies such as cracking or delamination. These simplifications may lead to discrepancies between simulated and experimental spectra in highly damaged regions.

## 5. Conclusions

This study investigated the scattering spectral characteristics of triple-junction GaAs solar cells subjected to nanosecond pulsed laser irradiation to establish a foundation for remote laser damage assessment. The Bidirectional Reflectance Distribution Function (BRDF) in the 400–1200 nm range was measured for cells irradiated at varying energy densities. The results demonstrate a direct and quantifiable correlation between the laser energy density and the evolution of distinct spectral features. Quantitatively, the disappearance of oscillation features in the near-infrared spectrum occurred at a threshold of approximately 1.16 J/cm<sup>2</sup>, while the complete obliteration of visible-range absorption peaks was observed at 1.58 J/cm<sup>2</sup> and above.

By combining experimental measurements with a scattering spectrum model based on thin-film interference theory, the spectral changes were conclusively linked to layer-specific damage. It was found that the GaInP top cell governs the absorption characteristics in the visible spectrum, with increasing damage leading to a reduction in thickness, a decrease in the number of absorption peaks, and peak position shifts. Concurrently, the GaAs middle cell primarily influences the oscillation characteristics in the near-infrared spectrum, the disappearance of which signifies severe damage to this layer.

The implications of this study are threefold: First, it establishes the foundation for non-destructive, remote diagnostics of solar cell health via spectral analysis. Second, the insights into layer-specific vulnerabilities can inform the design of more radiation-hardened

and laser-resistant solar cells for future space missions. Third, the methodology has high potential for revealing damage mechanisms in multi-junction cells under various high-energy irradiation conditions. Compared to traditional methods such as optical microscopy or electrical performance testing, which require proximity or direct contact, our spectral methodology offers a unique advantage as a remote, non-contact diagnostic tool. While it may not replace high-resolution techniques like SEM for detailed morphological analysis, it provides a rapid and effective means for initial damage screening and severity classification from a distance. The demonstrated ability of spectral responses to act as damage indicators opens a pathway for real-time monitoring of solar panels in critical environments, such as in orbit.

While the spectral signatures are clear under controlled laboratory conditions, their detectability from orbit depends on sensor sensitivity, atmospheric conditions, and target illumination. The current agreement between the model and experiment is primarily qualitative; a comprehensive quantitative validation, including rigorous uncertainty analysis and RMSE evaluation across a larger sample set, is essential for developing a robust predictive tool and will be a central focus of subsequent research. Furthermore, while the layer-specific damage mechanism is strongly supported by the spectral model, direct experimental verification via cross-sectional microscopy is needed for definitive confirmation. Future work will therefore focus on (1) scaling the detection approach to realistic remote sensing scenarios, (2) integrating machine learning for automated damage classification, and (3) incorporating advanced microscopy (e.g., SEM, AFM) to directly correlate morphological changes with spectral signatures.

**Author Contributions:** Conceptualization, H.C. and W.Z.; methodology, H.C.; validation, W.Z.; formal analysis, W.Z.; investigation, W.Z.; resources, H.C. and W.Z.; data curation, W.Z., Z.J., Y.M. and C.X. (Can Xu); writing—original draft preparation, W.Z. and H.C.; writing—review and editing, H.C.; visualization, Z.J. and C.X. (Chenyu Xiao); funding acquisition, H.C. and W.Z. All authors have read and agreed to the published version of the manuscript.

**Funding:** This research was funded by the National Natural Science Foundation of China under Grant Nos. 11602304 and 11502301.

**Institutional Review Board Statement:** Not applicable.

**Informed Consent Statement:** Not applicable.

**Data Availability Statement:** The data presented in this study are available on request from the corresponding author.

**Acknowledgments:** The authors would like to acknowledge C.X. for the assistance with the experiments.

**Conflicts of Interest:** The authors declare no conflicts of interest.

## References

1. Guo, W.; Chang, H.; Yu, C.H.; Li, M.Y. Damage characteristics of continuous-wave laser ablation triple-junction solar cells. *J. Laser Appl.* **2022**, *34*, 042038. [[CrossRef](#)]
2. Guo, W.; Chang, H.; Xu, C.; Zhou, W.J.; Yu, C.H.; Ji, G. Effect of Continuous Laser Irradiation on Scattering Spectrum Characteristics of GaAs Cells. *Spectrosc. Spectr. Anal.* **2023**, *43*, 3647–3681.
3. Qian, F.; Shen, H.; Huang, G.; Liu, B.; Hong, J. Improvement of Laser-Induced Damage on High-Efficiency Solar Cells via Top-Hat Beam Ablatio. *Energies* **2024**, *17*, 858. [[CrossRef](#)]
4. Li, S.; Huang, L.; Ye, J.; Hong, Y.; Wang, Y.; Gao, H.; Cui, Q. Study on Radiation Damage of Silicon Solar Cell Electrical Parameters by Nanosecond Pulse Laser. *Electronics* **2024**, *13*, 1795. [[CrossRef](#)]
5. Taylor, J.D. *Introduction to Ultra-Wideband Radar Systems*; CRC Press eBooks: Boca Raton, FL, USA, 2020.
6. Li, C.; Tan, Y.; Liu, C.; Guo, W. Rice Origin Tracing Technology Based on Fluorescence Spectroscopy and Stoichiometry. *Sensors* **2024**, *24*, 2994. [[CrossRef](#)] [[PubMed](#)]

7. Xu, C.; Zhang, Y.S.; Zhao, Y.S.; Li, P. Advances in Spectroscopic Characters of Space Object. *Spectrosc. Spectr. Anal.* **2017**, *37*, 672–678.
8. Jorgensen, K.M. *Using Reflectance Spectroscopy to Determine Material Type of Orbital Debris*; University of Colorado at Boulder: Boulder, CO, USA, 2000.
9. Jorgensen, K.; Africano, J.; Hamada, K.; Stansbery, E.; Sydney, P.; Kervin, P. Physical properties of orbital debris from spectroscopic observations. *Adv. Space Res.* **2004**, *5*, 1021–1025. [[CrossRef](#)]
10. Bedard, D.; Lévesque, M. Analysis of the CanX-1 engineering model spectral reflectance measurements. *J. Spacecr. Rocket.* **2014**, *5*, 1492–1504. [[CrossRef](#)]
11. Bedard, D.; Wade, G.A.; Abercromby, K. Laboratory characterization of homogeneous spacecraft materials. *J. Spacecr. Rocket.* **2015**, *4*, 1038–1056. [[CrossRef](#)]
12. Bedard, D.; Wade, G.A. Time-resolved visible/near-infrared spectrometric observations of the Galaxy 11 geostationary satellite. *Adv. Space Res.* **2017**, *1*, 212–229. [[CrossRef](#)]
13. Li, P.; Li, Z.; Xu, C.; Fang, Y.Q. Research on the Scattering Spectrum of GaAs-Based Cell Based on Thin-Film Interference Theory. *Spectrosc. Spectr. Anal.* **2020**, *10*, 3092–3097.
14. Das, N.; Chandrasekar, D.; Nur-E-Alam, M.K.K.; Khan, M.M. Light Reflection Loss Reduction by Nano-Structured Gratings for Highly Efficient Next-Generation GaAs Solar Cells. *Energies* **2020**, *13*, 4198. [[CrossRef](#)]
15. Das, N.; Sharma, A.; Basher, M.K.; Nur-E-Alam, M. Simulation and Optimization of Nano-structured Gratings Alternative of Thin-film Anti-Reflectors for GaAs Solar Cells Conversion Efficiency Improvement. In Proceedings of the 2022 International Conference on Numerical Simulation of Optoelectronic Devices (NUSOD), Turin, Italy, 12–16 September 2022; pp. 213–214.
16. Nur-E-Alam, M.; Yap, B.K.; Kiong, T.S.; Basher, M.K.; Abedin, T.; Islam, M.A.; Ibrahim, M.A.; Khandaker, M.U.; Das, N. Enhancing GaAs solar cell efficiency through nanostructured features: A comprehensive review of recent advances, challenges and future outlook. *Inorg. Chem. Commun.* **2025**, *178*, 114523. [[CrossRef](#)]

**Disclaimer/Publisher’s Note:** The statements, opinions and data contained in all publications are solely those of the individual author(s) and contributor(s) and not of MDPI and/or the editor(s). MDPI and/or the editor(s) disclaim responsibility for any injury to people or property resulting from any ideas, methods, instructions or products referred to in the content.